SPECTROSCOPIC MEASUREMENTS ON AN H⁻ ION SOURCE DISCHARGE[*]

Roderich Keller[†] and H. Vernon Smith, Jr., AT-2, MS H818
Los Alamos National Laboratory, Los Alamos, NM 87545 USA

Summary

Spectral emission lines from an H⁻ Penning surface-plasma source (SPS), the 4X source, are examined in the visible and near ultraviolet. Electron distribution temperatures are deduced from integral line-strength measurements. These temperatures are surprisingly low, about 0.5 eV. Electron density values of about 1.5×10^{14} cm⁻³ and H-atom energies between 2 and 2.6 eV are determined from the measured Balmer-line profiles. Assuming the H⁻ energy is identical to the H-atom energy, an emittance limit of 0.006 π·cm·mrad is deduced for this source with a 5.4-mm aperture.

Introduction

The SPS provides bright H⁻ beams for accelerator applications.[1] Not much is known about the plasma parameters of the source, but such information may prove quite valuable in theoretical modeling and in understanding the performance limits. The primary aim of our experiment is to use quantitative plasma spectroscopy to determine the transverse H⁻ ion energy that, along with the aperture size, sets a lower limit for the source emittance. Our experimental techniques and interpretation of the measurements follow standard procedures described in textbooks.[2,3] Hydrogen-atom energies are determined from the Doppler broadening of the H_α linewidth, and electron densities from the Stark broadening of the H_β and H_δ linewidths. Electron distribution temperatures are calculated from the intensity ratios of molybdenum, cesium, and hydrogen lines. A more detailed description of the experimental apparatus, measured data, and derived quantities is given elsewhere.[4]

Experimental Apparatus and Method

The 4X source is a Penning SPS, described in detail elsewhere.[5] Figure 1 shows the experimental setup. The plasma column is observed side-on through the 4.4-mm-diam ion extraction aperture. The emitted light passes through a quartz vacuum window and is imaged with slight demagnification onto the monochromator entrance slit. The lens transmission is sufficient for wavelengths down to 350 nm. The monochromator slits are perpendicular to the source magnetic field axis. The sensitivity of the whole system, including the photomultiplier, is calibrated by measuring the known spectral emission of a 100-W tungsten/halogen lamp.

Line profiles are measured at 20-μm slit widths where the measured instrument profile is Gaussian, with a full half-width of 0.011 nm. All measurements are time-resolved but are averaged over 10-20 discharge pulses, and high-frequency oscillations are smoothed out. Interestingly enough, even for quiescent discharge conditions (H⁻ current-signal noise level about 1% for 50-MHz bandwidth), the integral line-intensity signals show strong oscillations: ±20% for H_α, ±70% for Cs II, and ±10% for Mo I at 1-MHz bandwidth (the Cs II signal is shown in Fig. 2b).

For all examined discharge conditions, the ion current delivered by the source is measured with a Faraday cup inserted 5 cm from the source. During the spectroscopic measurements, the cup is removed and no
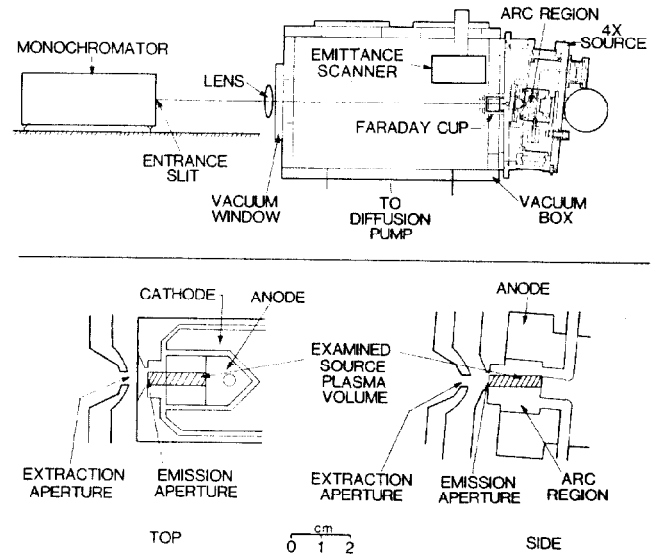
Figure 1. Upper: experimental arrangement of the 4X source and the 1-m monochromator on the ion source test stand (not to scale). The distance from the emission aperture to the lens is 67 cm; to the monochromator, 107 cm. Lower: horizontal (top) and vertical (side) sections of the 4X source plasma volume. Only a small portion (cross-hatched area) of the arc region is examined with the monochromator.
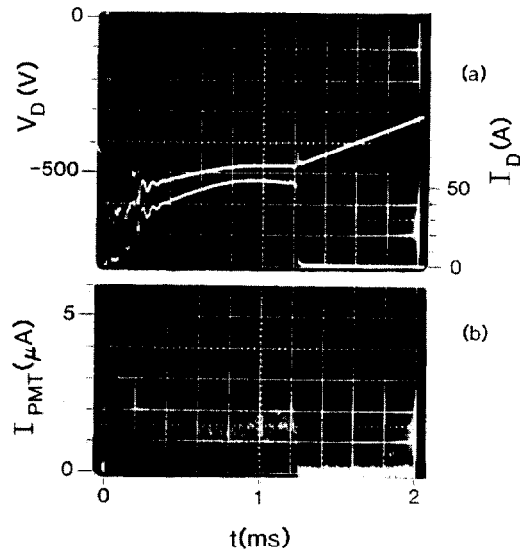

Figure 2. Oscillograms for Condition III, of (a) discharge voltage V_D (upper) and current I_D (lower); and (b) the photomultiplier tube current I_{PMT} for the Cs II line at 460.38 nm. The oscilloscope bandwidth is 50 MHz for V_D and 1 MHz for the other signals.

extraction voltage is applied. Four different discharge conditions are investigated: a noisy mode (I) with 300 V and 80 A, yielding 90 mA of H⁻ ions at 29 kV, with 1.5-ms pulse width at 5-Hz repetition rate; a low-voltage mode (II) with 130 V, 180 A, and 1.2 ms, yielding 100 mA of H⁻ at 29 kV; a quiescent mode (III) with 480 V, 55 A, 1.2 ms, and 60 mA of H⁻ at 21 kV; and, last, a dc mode (IV) at much reduced instantaneous power with 270 V and 1.06 A, yielding about 1 mA of H⁻ ion current at 5 kV.

Calculation of Plasma Parameters

For lines of one ionization state of an element, the electron temperature of the plasma is determined from the intensity ratio by using the formula $kT_e = (E_j-E_i)/\ln[(A_jg_j\lambda_iI_iK_i)/(A_ig_i\lambda_jI_jK_j)]$, with j the line emitted from an upper level of higher excitation energy E than line i; A the transition probabilities; g the statistical weights; λ the wavelengths; I the recorded integral intensities; and K the calibration factors. A true electron temperature is represented by kT_e only in the case of local thermodynamical equilibrium (LTE). If LTE cannot be verified, there may be different kT_e values, depending on the energy values of the levels involved, and kT_e then means the distribution temperature.

The emission lines used in deriving the source plasma parameters are listed in Table I. Wavelengths, statistical weights, and level energies are taken from the tables in Refs. 6 and 7. Transition probabilities are found in a recent review[8] and monographs for molybdenum[9] and for cesium.[10] No transition probabilities for singly ionized cesium are available; therefore, lifetime data[11] of excited Cs II levels are used, and the transition probabilities of the Cs ion lines are assumed to be one-tenth of the inverse lifetimes of the radiating levels.

TABLE I
DATA OF SPECTRAL LINES
USED TO DERIVE PLASMA PARAMETERS

	λ(nm)	E(eV)	A·g(10^8s^{-1})
H_α	656.28	12.09	4.19
H_β	486.13	12.75	1.43
H_δ	410.17	13.22	0.389
Cs I	455.53	2.72	0.0859
Cs I	672.33	3.23	0.273
Cs I	728.00	3.51	0.491
Cs II	460.38	16.01	6.6[a]
Cs II	522.70	15.68	2.2[a]
Mo I	379.83	3.26	6.09
Mo I	386.41	3.20	4.57
Mo I	390.30	3.17	3.25
Mo I	506.25	5.03	0.213
Mo I	516.78	5.08	0.64
Mo I	525.90	4.94	0.74

[a]Transition probability calculated from level lifetime as discussed in the text.

Measured line profiles result from a convolution of the different shapes that are due to linear Stark broadening, related to the electron density; Doppler broadening, caused by the motion of radiating atoms; instrument profile; and the fine-structure splitting of the sublevels. For H_α profiles, a fine-structure correction curve is calculated following the procedure mentioned in Ref. 12, considering all seven sublevel positions. The fine-structure correction is negligible for the other Balmer-series profiles.

To separate Stark and Doppler broadening, a general tendency can be exploited: Doppler broadening scales proportionally to the wavelength of the observed line;[2] thus, H_α shows the largest Doppler broadening effect of the lines we examine. Stark broadening is larger for H_β and H_δ than for H_α and H_γ. Therefore, H_α and H_γ are better suited for atomic temperature determinations, and H_β and H_δ are better for electron density measurements.

For determining the H-atom temperature, we use only the H_α linewidth because H_γ Stark-broadening parameters are published in Ref. 2 down to electron densities of only 1×10^{15} cm^{-3}. Extrapolation of the tabulated values to 1×10^{14} cm^{-3} could lead to large errors in the value derived for the Doppler width because the

extrapolated values of the H_γ Stark and Doppler widths are roughly equal. Examples of the measured profiles of H_α and H_δ, together with ideal Gaussian or Lorentzian profiles of equal half-width, are shown in Fig. 3.
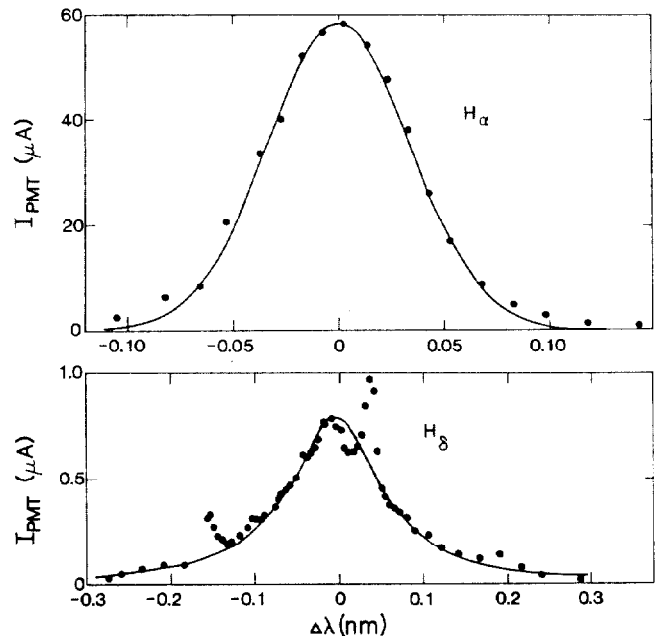

Figure 3. Profiles of the H_α (upper) and H_δ (lower) Balmer lines. The dots are the data. The Gaussian (upper) and Lorentzian (lower) curves have the same half-widths as the measured profiles. H_2 and Mo lines are mixed in the H_δ profile.

The actual defolding procedure uses the tabulated Voigt function parameters.[3] Knowing the total width and the width of either a Gaussian or a Lorentzian profile, one can immediately look up the width of the other profile. Hydrogen Stark profiles have nearly Lorentzian shapes, whereas Doppler- and instrument-broadening effects produce Gaussian shapes. The instrument profile half-width is subtracted from the Doppler-broadening half-width by assuming they add quadratically. Measured line widths, derived electron densities, H-atom energies, and electron distribution temperatures are shown in Table II.

TABLE II
DERIVED PLASMA PARAMETERS

Discharge mode[a]	I	II	III	IV
H_α measured full half-width, nm	0.0725	0.0825	0.0800	0.0350
H_β measured full half-width, nm	0.083	0.0925	0.0970	0.0325
Electron density, 10^{14} cm^{-3}	1.08	1.29	1.66	0.2[b]
H-atom energy, eV	2.0	2.6	2.3	0.27
Electron distribution temperatures, eV				
From Mo I	0.49	0.50	0.55	1.02
From Cs I	--	0.50	--	0.28
From Cs II	0.72	0.93	0.72	0.35
From H I	--	--	0.33[c]	--

[a]Discharge mode: See text.
[b]Uncertain because the Stark parameter was extrapolated.
[c]Measured line profiles are graphically integrated.

Discussion of the Results

The most striking feature of the derived plasma parameters (Table II) is that the Mo-based electron distribution temperatures have small deviations from

their average, even though the pulsed discharge Conditions I-III are considerably different, and are always considerably lower than the H-atom energies (except for the dc case). Plasma turbulence effects may cause these higher H-atom energies. Strong oscillations of the line intensity signals, even with quiescent discharge voltage and current signals (Fig. 2), support this view. The most likely explanation for the significant deviations between the electron temperatures derived from different atom or ion species is that the electron energy distributions are non-Maxwellian. The small size of the variations of the derived electron density values is also surprising because the discharge currents vary by up to a factor of 3.3 for Conditions I-III. This unexpected behavior may be largely due to the fact that the measurements are performed integrating over the spatial depth of the discharge (Fig. 1) and smoothing out all time-dependent variations with frequencies higher than 10 kHz.

To evaluate particle density ratios, the LTE state must be confirmed. Applying Saha's equation[2] to cesium at the measured electron temperature (0.55 eV) and density for discharge Condition III, we get an expected Cs^+/Cs^0 density ratio of 6.6 x 10^3. However, the Boltzmann formula with 0.55-eV electron temperature requires a Cs^+/Cs^0 density ratio 10^6 times larger than the Saha result to explain the CsII/CsI (λ = 460 and 455 nm) line intensity ratio. An assumed temperature of 0.93 eV would yield equal values of the Cs^+/Cs^0 ratio for the Saha and Boltzman calculations, but all electron temperature measurements for Condition III show significantly lower values. Thus, the conclusion is that the plasma is not in the LTE state, and probably a second population of electrons with higher energies than those corresponding to a Maxwellian distribution for 0.55-eV temperature causes the disagreement. In this situation, it is not justified to derive quantitative particle-density ratios for the source discharge plasma.

A calculation of the relaxation time for the energy exchange between H-atoms and H^- ions yields about 1 x 10^{-7} s, assuming an atom density of 1 x 10^{15} cm^{-3} and a collision cross section of 5 x 10^{-15} cm^2 (Ref. 13). The corresponding mean free path is 0.2 cm, about ten times less than the source discharge-chamber dimensions, which supports our assumption that the H^- ions have the same energies as the H atoms.

For a Maxwellian ion distribution of energy kT, the emittance versus beam fraction for a circular aperture has been calculated.[14] The 2-D normalized rms emittance is given by $\varepsilon_{x,y} = (kT/mc^2)^{1/2} \cdot R/2$, where R is the aperture radius and mc^2 = 938 MeV. This rms emittance includes 39% of the beam particles. Table III gives the emittance values for each of the four discharge conditions, using the H-atom energy values of Table II for the H^- ion energy and R = 0.27 cm. The brightness B is calculated from B = $2I_-/(\pi^2 \varepsilon_x\varepsilon_y)$, using the total measured H^- current I_-. For comparison with these calculated values, the measured values[5] for Conditions I, II, and III are also given in the last four lines of Table III.

TABLE III
EMITTANCE, CURRENT, AND BRIGHTNESS VALUES

Discharge Mode	I	II	III	IV
$\varepsilon_{x,y}(\pi \cdot cm \cdot mrad)$[a]	0.0062	0.0071	0.0067	0.0023
$I_-(mA)$[b]	90	100	60	1
$B(A/cm^2 \cdot mrad^2)$[a]	480	410	270	39
$\varepsilon_x(\pi \cdot cm \cdot mrad)$	0.017	0.022	0.011	--
$\varepsilon_y(\pi \cdot cm \cdot mrad)$	0.018	0.023	0.012	--
$I_-(mA)$	110	100	67	--
$B(A/cm^2 \cdot mrad^2)$	72	40	103	--

[a]Calculated
[b]Measured

The measured emittances for the examined beams are considerably larger than the emittances calculated using the H-atom energies; therefore, either the H^- ion energies are much higher than the H-atom energies or other effects contribute significantly to the measured emittances. These possible sources of emittance include aberrations in the extraction system, magnetic dispersion of the H^- ions, increase in the time-averaged emittance caused by perveance fluctuations in the extraction gap, or nonlinear space-charge compensation effects. Thus, it may be possible to reduce the emittance and increase the brightness of the source by reducing or eliminating one or more of these other effects.

Conclusions

The plasma parameters of the pulsed discharge in the 4X source are H-atom energy, 2-2.6 eV; electron density, 1-1.7 x 10^{14} cm^{-3}; and electron temperature, ~0.5 eV. If, as seems likely, the value of the H^- energy is equal to the H-atom energy, the lower limit for the 4X source's pulsed H^- beam emittance is 0.006 $\pi \cdot cm \cdot mrad$ for a 0.54-cm aperture.

Acknowledgments

References

1. G. E. Derevyankin and V. G. Dudnikov, "Production of High Brightness H^- Beams in Surface-Plasma Sources," AIP Conf. Proc. No. 111, AIP, New York (1984), 376.
2. H. R. Griem, Plasma Spectroscopy, (McGraw-Hill, New York, 1964).
3. W. Lochte-Holtgreven, Ed., Plasma Diagnostics, (North Holland Publ. Co., Amsterdam, 1968), esp. Vols. 1, 2, 3, 5.
4. R. Keller and H. V. Smith, Jr., "Spectroscopic Measurements on an H^- Ion Source Discharge," Los Alamos National Laboratory ATS Tech. Note AT-2-ATS-7 (1985).
5. H. V. Smith, Jr., P. Allison, and J. D. Sherman, "A Scaled, Circular Emitter Penning SPS for Intense H^- Beams," AIP Conf. Proc. No. 111, AIP, New York (1984), 458; and "The 4X Source," these proceedings.
6. A. R. Striganov and N. S. Sventitskii, Tables of Spectral Lines of Neutral and Ionized Atoms, (IFI/Plenum, New York, 1968).
7. A. N. Saidel, V. K. Prokof'ev, and S. M. Raiski, Spektraltabellen, (VEB Verlag Technik, Berlin, 1961).
8. J. Reader, C. H. Corliss, W. L. Wiese, and G. A. Martin, "Wavelengths and Transition Probabilities for Atoms and Atomic Ions," National Bureau of Standards, Washington, DC, report NSRDS-NBS-68 (1980).
9. S. E. Schnehage, K. Danzmann, R. Kuennemeyer, and M. Kock, "Oscillator Strengths of Neutral and Singly Ionised Molybdenum," J. Quant. Spectrosc. Radiat. Transfer 29 (1983), 507; E. L. Nikonova and V. K. Prokof'ev, "The Ratio of the Oscillator Strengths of Components of the Resonance Multiplets of Al, Tl, Cr, Mn, Mo, and Ions of Ba, Ca, and Sr," Optika I Spektroskopiya 1 (1956), 290; and N. N. Kirsanova, "The Absolute Transition Probabilities for the Molybdenum Lines," Zh. Prikl. Spektrosk. 15 (1971), 536.
10. W. B. Hawkins, "Cesium Transition Probabilities for Optical Pumping," Phys. Rev. 123 (1962), 544; C. L. Chen and A. V. Phelps, "Absorption Coefficients for the Wings of the First Two Resonance Doublets of Cesium Broadened by Argon," Phys. Rev. A7 (1973), 470; and O. S. Heaves, "Radiative Transition Probabilities of the Lower Excited States of the Alkali Metals," J. Opt. Soc. Am. 51 (1961), 1058.
11. A. L. Osherovich and A. Ya. Nikolaich, "Radiation Lifetimes of Excited States of the Cesium Ion," Optika I Spektroskopiya 46 (1979), 639; and E. Alvarez, A. Arnesen, A. Bengtson, J. Campos, R. Hallin, C. Nordling, T. Noreland, and O. Staaf, "Hyperfine Structure and Life- time of Some Excited Levels in Cs^+," Phys. Rev. A21 (1980), 710.
12. M. W. Grossman, "H^- Ion Source Diagnostics," Proc. of Symp. on the Production and Neutralization of Negative Hydrogen Ions and Beams, Brookhaven National Laboratory report BNL-50727 (1977), 105.
13. D. L. Book, NRL Plasma Formulary, (Naval Research Laboratory, Washington, DC, 1978).
14. P. Allison, J. D. Sherman, and H. V. Smith, Jr., "Comparison of Measured Emittance of an H^- Ion Beam With a Simple Theory," Los Alamos National Laboratory report LA-8808-MS, (June 1981).